Available online at www.eccomasproceedia.org
Eccomas Proceedia COMPDYN (2025) 80- 88

ECCOMAS Proceedia

COMPDYN 2025
10th ECCOMAS Thematic Conference on
Computational Methods in Structural Dynamics and Earthquake Engineering
M. Papadrakakis, M. Fragiadakis (eds.)
Rhodes Island, Greece, 15-18 June 2025

CHARACTERIZATION OF THE PRESSURIZED-SAND DAMPERS WITH A NEWLY DEVELOPED UNIAXIAL MODEL

Konstantinos N. Kalfas[1], Nicolò Vaiana [2], and Nicos Makris[3]

[1] The University of Texas at Tyler
Dept. of Civil and Construction Engineering and Management, Tyler, TX 75799
e-mail: kkalfas@uttyler.edu

[2] University of Naples Federico II
Dept. of Structures for Engineering and Architecture, Napoli, IT, 80125
e-mail: nicolo.vaiana@unina.it

[3] Southern Methodist University
Dept. of Civil and Environmental Engineering, Dallas, TX 75205
nmakris@smu.edu

Abstract

This study presents the characterization of the recently developed pressurized sand damper (PSD) in which a steel sphere is moving within a cylindrical tube filled with sand that is under pressure. The experimental results presented in previous studies, revealed that the force output of the PSD is stable, symmetric and nearly velocity-independent; i.e., the PSD is a hysteretic response modification device. The component testing at various levels of pressure, stroke amplitude, and cycling frequency revealed an increasing pinching at larger strokes. The fidelity of a newly developed uniaxial phenomenological model, able to accurately simulate hysteretic phenomena in rate-independent systems is discussed. The newly developed Vaiana-Rosati model (VRM) requires only one history variable, and it does not need the solution of a differential equation for the evaluation of the generalized force. The VRM can capture the pronounced pinching of the PSD hysteretic behavior at larger stroke amplitudes when harmonic displacement loading is imposed, and it is also capable of producing symmetric force-displacement loops with pinching, when the input motion is a periodic displacement history with successive negative and positive displacement peaks that are not symmetric. The characterization of the PSD is assessed by comparing the obtained load-displacement loops from the experimental campaign with the VRM subjected different loading time-histories.

Keywords: Pressurized Sand Damper, Velocity-Independent Device, Pinched Hysteresis, Vaiana Rosati Model, Phenomenological Modeling.

Peer-review under responsibility of the organizing committee of COMPDYN 2025.
doi: 10.7712/120125.12659.25482

1 INTRODUCTION

The damping device industry experienced significant advancement over the last 50 years due to the increasing need for retrofitting schemes using response-modification devices. Seismic isolation [1, 2], supplemental damping and strength/ductility-oriented designs [3-5] are used extensively to increase the seismic design capacity of structures. Motivated partly by the need to develop sustainable energy dissipation devices that do not suffer from oil leakage due to failure of their end seals [6], and partly from the need to develop a robust damper that consists only of traditional civil engineering materials (sand and steel) in association with the use of post-tensioned steel rods with which practitioner civil engineers are familiar, a pressurized sand damper (PSD) which does not suffer from the challenges of viscous heating and addresses the quest for long-stroke, in association with rate-independent dissipation has been recently proposed [7-17]. Figure 1 shows a schematic of a PSD in which energy is dissipated due to the shearing action of the pressurized sand, where the shearing forces dominate over the inertia forces of the sand grains. The performance of the PSD can be continuously monitored with commercially available strain gauges that are installed along the post-tensioned steel rods that exert the desirable nominal pressure.

The phenomenological models are widely accepted as strong mathematical tools that explain accurately the hysteresis of inelastic systems, can provide a suitable description and generalization of experimental findings and are also used extensively for design purposes. For the past half century, multiple phenomenological models have been developed to account for the hysteretic representation of mechanical systems, such as the Ramberg -Osgood model [18], the Giuffrè-Menegotto-Pinto model [19], the widely used Bouc-Wen model [20-22], the Ozdemir model [23], and the recently developed Vaiana-Rosati [24-26] one. While initially, most of the phenomenological models were developed to represent a specific type of hysteresis of inelastic systems, later they were further extended to describe additional phenomena that appear in a system, and as such, their mathematical forms are nowadays suitable for multi-disciplinary extensions.

The Vaiana-Rosati model (VRM) [25-29] is used in this study to simulate the rate-independent response of the PSDs characterized by acute pinching phenomena [7-17]. The VRM belongs to a class of phenomenological models that can simulate hysteretic loops that are limited by two parallel lines/ curves of typically rate-independent systems. The VRM appears to be a more computationally efficient class model of algebraic or exponential nature since the output variable is evaluated in a closed-form. This results in significantly reduced computational time for geometrically and mechanically non-linear dynamics analyses, and it can accurately describe complex hysteresis loops, such as the pinched ones.

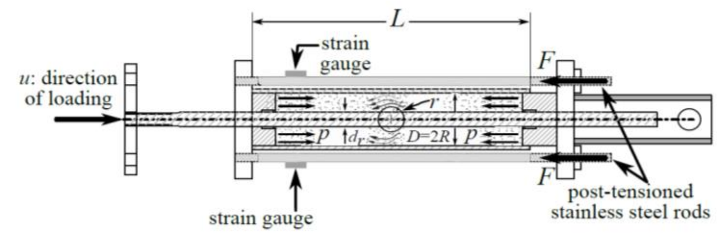

Figure 1: Schematic of the proposed PSD. The pressure applied to the enclosed sand is illustrated through a diagram of forces. (Adapted from [17].)

2 PSD EXPERIMENTAL CAMPAIGNS UNDER CONSIDERATION

Two different experimental campaigns are used to simulate the hysteretic rate-independent behavior of PSDs with the VRM. One is conducted in the Structures Laboratory at Southern Methodist University with a sphere appended on the piston-rod; and one is conducted in the Natural Hazards Engineering Research Infrastructure (NHERI) Lehigh Experimental Facility (EF) at Advanced Technology for Large Structural Systems (ATLSS) Engineering Research Center, at Lehigh University [17, 30, 31], where the sphere appended on the piston-rod of the PSDs is merely replaced with a bolt of 1.27 cm diameter with the bolt-head and nut protruding from each side of the piston-rod as shown in Fig. 2. The latter is discussed in details in the recent study by Kalfas *et al.* [17].

2.1 PSD with a sphere appended on the piston-rod

Different configurations have been used for this experimental campaign. These configurations have been obtained by assembling damper housings (cylindrical tubes) of L= 60.96 and 68.58 cm length, and diameters of D= 2R= 12.38 and 13.97 cm; while the spheres appended on the piston-rod had diameters of d= 2r= 5.080 and 5.715 cm, with the piston-rod diameter being d_r= 3.175 cm. The PSDs have been filled with dry sand of different sand grains size of aggregation gradation 0.07 mm < d_{gr} < 2.25 mm.

2.2 PSD with the bolt-head and nut protruding from each side of the piston-rod

In order to delay the manifestation of the pinching effect at longer displacements, and to avoid the attraction of unnecessary large forces due to pinching, that is, to generate a milder pinching, the sphere appended on the piston-rod of the PSDs is merely replaced with a 1.27 cm diameter bolt with the bolt-head and nut protruding from each side of the piston-rod. This experimental campaign took place in the NHERI Lehigh EF at ATLSS Engineering Research Center, at Lehigh University.

This configuration consists of a damper housing (cylindrical tube) of L= 60.96 cm length and D= 2R= 11.43 cm internal diameter, while the piston-rod diameter was d_r= 3.18 cm. The damper housing has been filled with dry sand of an average density of $\rho \approx$ 1,900 kg/m^3 and an aggregation gradation range of 0.6 < d_{gr} < 2 mm.

Figure 2: Piston rods used in the pressurized sand damper where the mounted sphere has been replaced with a 1.27 cm diameter bolt. (Adapted from [11].)

3 THE VAIANA ROSATI MODEL (VRM)

3.1 VRM+A formulation

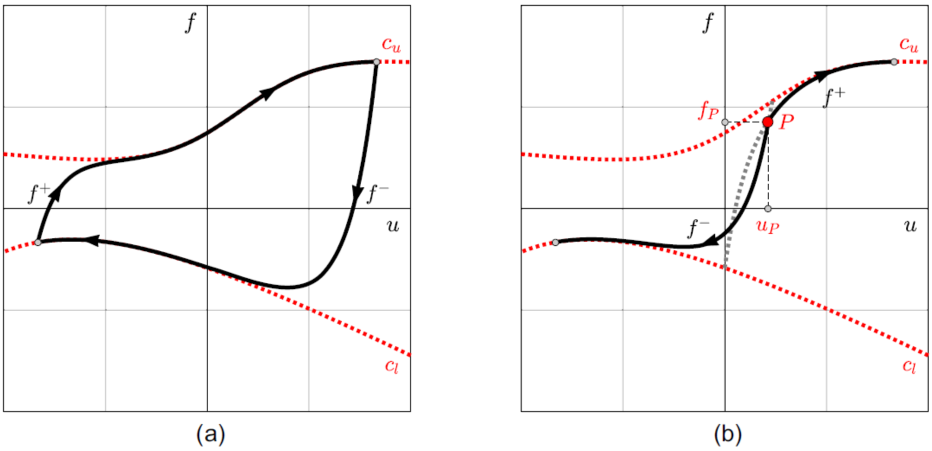

Figure 3: VRM formulation: (a) curves describing a generic force-displacement hysteresis loop; and (b) generic point P of the response. (Reprinted from Mechanical Systems and Signal Processing, Vol. 199, N. Vaiana and L. Rosati "Analytical and differential reformulations of the Vaiana–Rosati model for complex rate-independent mechanical hysteresis phenomena," 110448, © 2023, with permission from Elsevier.)

The analytical, VRM+A, form [27] does not need the evaluation of an internal variable, and as such it simplifies its implementation in computer programs, allowing for its use in design procedures.

The VRM+A describes a generic force-displacement hysteresis loop by means of two curves; that is, the generic loading f^+ and unloading f^- curves, as shown in Fig. 3a. The former (latter) asymptotically approaches the upper (lower) limiting curve c_u (c_l).

Particularly, the equation of f^+ is:

$$f^+(u, u_P, f_P) = f_e^+(u) + k_b^+ u + f_0^+ - (f_e^+(u_P) + k_b^+ u_P + f_0^+ - f_P)e^{-\alpha^+(u-u_P)} \tag{1}$$

with:

$$f_e^+(u) = \beta_1^+ e^{\beta_2^+ u} - \beta_1^+ + \frac{4\gamma_1^+}{1 + e^{-\gamma_2^+(u-\gamma_3^+)}} - 2\gamma_1^+ \tag{2}$$

The corresponding equation of f^- is:

$$f^-(u, u_P, f_P) = f_e^-(u) + k_b^- u - f_0^- - (f_e^-(u_P) + k_b^- u_P - f_0^- - f_P)e^{+\alpha^-(u-u_P)} \tag{3}$$

with:

$$f_e^-(u) = \beta_1^- e^{\beta_2^- u} - \beta_1^- + \frac{4\gamma_1^-}{1 + e^{-\gamma_2^-(u-\gamma_3^-)}} - 2\gamma_1^- \tag{4}$$

where, u is the applied displacement, u_P and f_P are the coordinates of the current point P of the response as shown in Fig. 3b, and the other terms are the model parameters, which are discussed in details in Kalfas et al. [17].

3.2 VRM+D formulation

The VRM+D adopts equivalent rate equations for the simulation of the generic force-displacement hysteresis loop illustrated in Fig. 3a. In particular, f^+ is evaluated by solving the following first-order ordinary differential equation:

$$\dot{f}^{+}(u,u_P,f_P) = [k_e^{+}(u) + k_b^{+} + \alpha^{+}(f_e^{+}(u) + k_b^{+}u + f_0^{+} - f^{+}(u,u_P,f_P))]\dot{u} \quad (5)$$

in which $f_e^{+}(u)$ is given by Equation (2), and:

$$k_e^{+}(u) = \frac{d}{du}f_e^{+}(u) = \beta_1^{+}\beta_2^{+}e^{\beta_2^{+}u} + \frac{4\gamma_1^{+}\gamma_2^{+}e^{-\gamma_2^{+}(u-\gamma_3^{+})}}{[1+e^{-\gamma_2^{+}(u-\gamma_3^{+})}]^2} \quad (6)$$

Similarly, f^{-} is computed by solving:

$$\dot{f}^{-}(u,u_P,f_P) = [k_e^{-}(u) + k_b^{-} - \alpha^{-}(f_e^{-}(u) + k_b^{-}u - f_0^{-} - f^{-}(u,u_P,f_P))]\dot{u} \quad (7)$$

where $f_e^{-}(u)$ is given by Equation (4), and:

$$k_e^{-}(u) = \frac{d}{du}f_e^{-}(u) = \beta_1^{-}\beta_2^{-}e^{\beta_2^{-}u} + \frac{4\gamma_1^{-}\gamma_2^{-}e^{-\gamma_2^{-}(u-\gamma_3^{-})}}{[1+e^{-\gamma_2^{-}(u-\gamma_3^{-})}]^2} \quad (8)$$

In the previous equations, the overdot denotes differentiation with respect to time.

3.3 Simulation with the VRM of a response to periodic, asymmetric input variables

To demonstrate the model capacity to simulate pinched hysteresis loops also when the input motion is a periodic displacement time-history with nonsymmetric, successive negative and positive peaks, let us consider the displacement time-history illustrated in Fig. 4a, which is analytically described by the following equation:

$$u(t) = u_0[\sin(\omega_1 t) + \sin(\omega_2 t)] \quad (9)$$

where $\omega_1 = 2\pi/T_1 = 2\pi/0.2$s and $\omega_2 = 2\pi/T_2 = 2\pi/0.3$s represent two distinct circular frequencies.

Figure 4b shows the hysteresis loops obtained by imposing the described periodic input variable and adopting the model parameters listed in Table 1. It is evident that the model can properly reproduce pinched hysteresis loops even when the imposed displacement time-history is characterized by asymmetric successive positive and negative peaks.

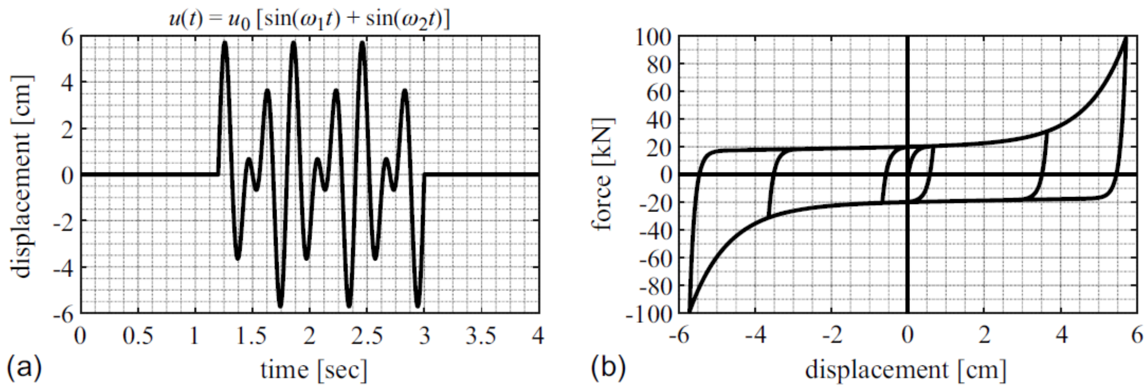

Figure 4: (a) Applied displacement time-history characterized by asymmetric successive positive and negative peaks; and (b) hysteresis loops obtained by using the model parameters in Table 1. (Adapted from [17].)

sgn ($\dot{u}$)	k_b (kN/cm)	f_0 (kN)	a (1/cm)	β_1 (kN)	β_2 (1/cm)	γ_1 (kN)	γ_2 (1/cm)	γ_3 (cm)
+	0.5	20	7.5	+0.25	+1	0	0	0
-	0.5	20	7.5	-0.25	-1	0	0	0

Table 1: Model parameters adopted for simulating the hysteresis loops in Fig. 4b.

4 SIMULATION OF THE PSD RESPONSE TO PERIODIC DISPLACEMENT TIME-HISTORIES WITH THE VRM

Figure 5 illustrates the comparisons among the experimental force-displacement hysteresis loops, normalized relative to the PSD strength, that is, $F_{SD}(u=0)$ [10, 11], and those reproduced by the VRM+A adopting the parameters given in Table 2. The responses in Fig. 5 are those obtained for the PSDs having L= 60.96 cm. The experimental responses (black solid

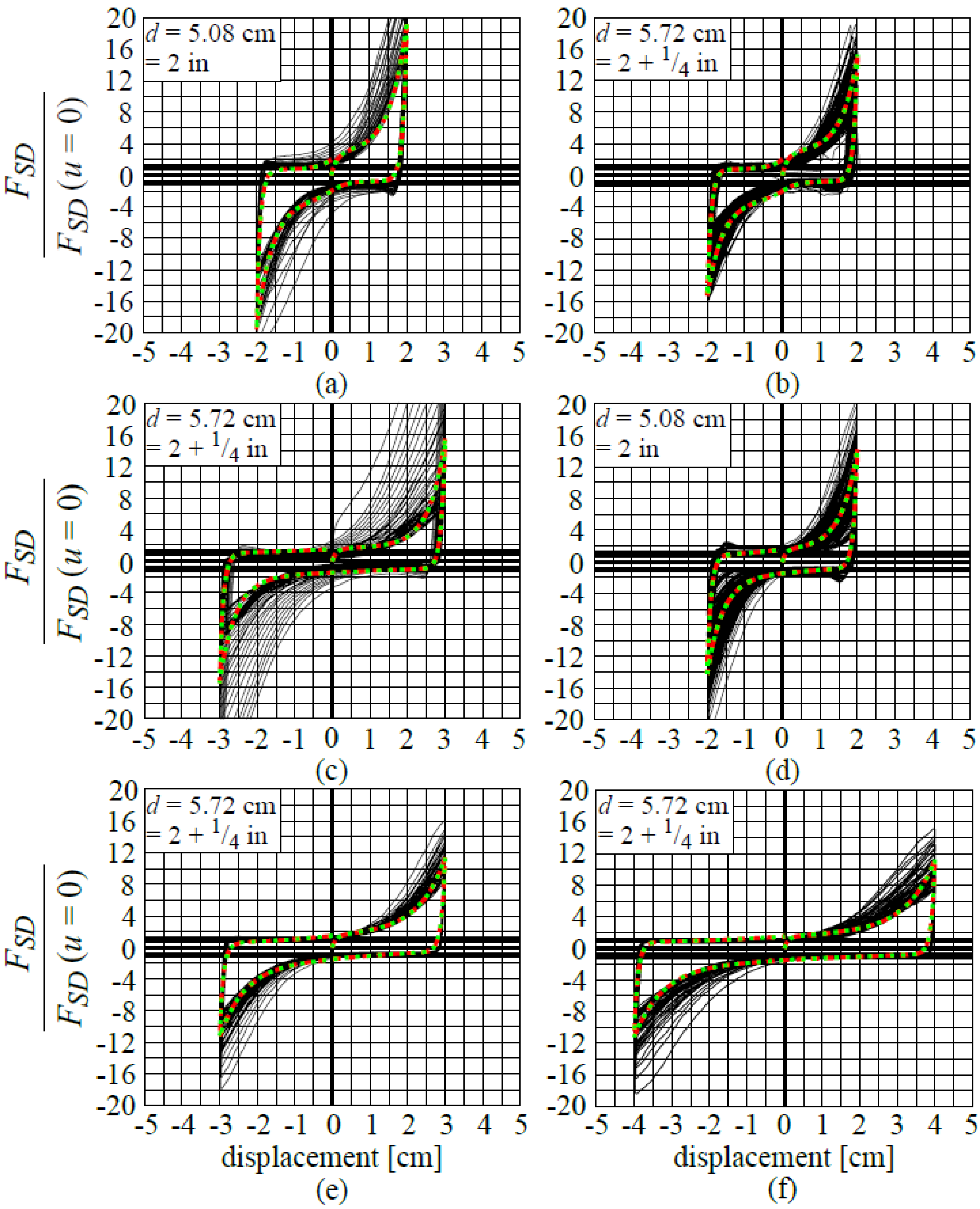

Figure 5: Simulation of normalized force-displacement loops to the strength of the PSDs: $F_{SD}(u=0) = \Pi_S\, p\, r^2 + \mu\, k\, p\, \pi\, d_{rod}\, L_{net}$ recorded at all exerted pressures, all cyclic frequencies and various stroke amplitudes with the Vaiana-Rosati model for L= 60.96 cm. The hysteretic model is predicted with f_0= 0.10 Hz and f_0= 10.0 Hz. [a-c]: D= 12.38 cm; [d-f]: D= 13.97 cm. (Adapted from [10].)

Fig.	sgn ($\dot{u}$)	k_b (N/m)	f_0 (N)	a (1/m)	β_1 (N)	β_2 (1/m)	γ_1 (N)	γ_2 (1/m)	γ_3 (m)
	+	0.1	2	10	+0.15	+2.35	0	0	0
5a	-	0.1	2	10	-0.15	-2.35	0	0	0
	+	0.1	2	10	+0.1	+2.4	0	0	0
5b	-	0.1	2	10	-0.1	-2.4	0	0	0
	+	0.01	1.5	10	+0.01	+2.4	0	0	0
5c	-	0.01	1.5	10	-0.01	-2.4	0	0	0
	+	0.1	1.5	10	+0.1	+2.4	0	0	0
5d	-	0.1	1.5	10	-0.1	-2.4	0	0	0
	+	0.1	1.5	10	+0.1	+1.5	0	0	0
5e	-	0.1	1.5	10	-0.1	-1.5	0	0	0
	+	0.01	1.5	10	+0.05	+1.3	0	0	0
5f	-	0.01	1.5	10	-0.05	-1.3	0	0	0

Table 2: Values of the Vaiana-Rosati model parameters to generate the hysteretic loops in Fig. 5.

line), illustrated in each figure, have been obtained for the same displacement amplitude but for different values of pressure and frequency. We may note that the normalized force, $F_{SD}/F_{SD}(u=0)$, essentially lies along the ±1 solid horizontal black lines, validating the normalization and indicating the rate-independent nature of the PSDs. Similarly, the comparison between the simulated hysteresis loops obtained for a frequency of 0.10 Hz (red dashed line) with those obtained for a frequency of 10 Hz (green dotted line) reveals the rate-independent nature of the proposed model.

5 CONCLUSIONS

In this study, the complex nearly rate-independent behavior of the newly developed PSDs has been characterized by the recently formulated uniaxial hysteretic Vaiana-Rosati phenomenological class model. Simulations between the force-displacement loops normalized to the strength of the $F_{SD}\,(u=0) = \Pi_S\, p\, r^2 + \mu\, k\, p\, \pi\, d_{rod}\, L_{net}$, recorded at all exerted pressures, all cyclic frequencies and various stroke amplitudes and the Vaiana -Rosati model were presented. The recently developed Vaiana-Rosati model simulated with fidelity the complex rate-independent hysteretic loops exhibited by the proposed PSDs when the input motions were symmetric sinusoidal displacement histories. The recently developed Vaiana-Rosati model can also provide a closed-form solution for the evaluation of the proposed PSD response; it allows for accurate fitting of the hysteretic loops with the use of two sets of eight parameters to simulate the loading and unloading phases of hysteretic loops; it can simulate the response of the PSDs when subjected to earthquake input excitations; and it proves to be computationally-efficient.

REFERENCES

[1] J.M. Kelly, Aseismic base isolation: Review and bibliography. *Soil Dynamics and Earthquake Engineering*, **5**(**4**), 202-216. 1986.

[2] N. Makris, Seismic isolation: Early history. *Earthquake Engineering and Structural Dynamics*, **48**(**2**), 269-283. 2018.

[3] R.I. Skinner, J.M. Kelly, A.J. Heine, Hysteretic dampers for earthquake-resistant structures. *Earthquake Engineering and Structural Dynamics*, **3**(**3**), 287-296. 1974.

[4] T.T. Soong, G.F. Dargush, *Passive energy dissipation systems in structural engineering*. Willey, 1997.

[5] C.J. Black, N. Makris, I.D. Aiken, Component testing seismic evaluation and characterization of buckling restrained braces. *Journal of Structural Engineering*, **130**(**6**), 880-894, 2004.

[6] P. Matier, A. Ross, Bay bridge shock absorbers spring leak. *San Francisco Chronicle*, **20**, 2013.

[7] K.N. Kalfas, N. Makris, Estimation of the design parameters of pressurized sand dampers from experiments. *ASCE Engineering Mechanics Institute Conference (EMI2022)*. American Society of Civil Engineers: Baltimore, MD, May 31-June 3, 2022.

[8] U. El Shamy, E. Sabi, K.N. Kalfas, N. Makris, Characterization of energy dissipation during cyclic loading of a sand damper. *ASCE Engineering Mechanics Institute Conference (EMI2022)*. American Society of Civil Engineers: Baltimore, MD, May 31-June 3, 2022.

[9] K.N. Kalfas, N. Makris, Testing of the prototype and sustainable pressurized sand damper for the response modification of structures. *12th US National Conf. on Earthq. Eng.* Earthquake Engineering Research Institute: Salt Lake City, UT, June 27-July 1, 2022.

[10] K.N. Kalfas, *Component testing and characterization of an innovative pressurized sand damper for the response modification of structures*. (Ph.D. Thesis). Southern Methodist University, Dallas, TX, 2023.

[11] K.N. Kalfas, N. Makris, U. El Shamy U, Assessment of the effect of design parameters of pressurized sand dampers from component testing. *Journal of Engineering Mechanics*, **149**(**10**), 04023072, 2023.

[12] L. Cao, K.N. Kalfas, N. Makris, J. Ricles, Real-time hybrid simulation of a CLT rocking wall system equipped with pressurized sand dampers for seismic hazard mitigation. *ASCE Engineering Mechanics Institute Conference (EMI2023)*. American Society of Civil Engineers: Atlanta, GA, June 6-9, 2023.

[13] M. Karimipetanlar, U. El Shamy, K.N. Kalfas, N. Makris, The influence of particle shape on crushing pattern and energy dissipation within a pressurized sand damper. *Computers & Geotechnics*, **166**, 106020, 2024.

[14] M. Karimipetanlar, U. El Shamy, K.N. Kalfas, N. Makris, Numerical simulations of particle behavior and crushing within a pressurized sand damper subjected to cyclic loading. *Journal of Engineering Mechanics*, **150**(**1**), 04023106, 2024.

[15] K.N. Kalfas, N. Makris, Component testing of cost-effective pressurized sand-dampers. *18th World Conference on Earthquake Engineering (18WCEE)*. International Association of Earthquake Engineering: Milan, IT, June 3-July 5, 2024.

[16] K.N. Kalfas, N. Makris, Component testing of pressurized sand dampers to assess the effect of design parameters. *IABSE Congress San Jose 2024: Beyond Structural Engineering in a Changing World*. International Association for Bridge and Structural Engineering: San Jose, CR, September 25-27, 2024.

[17] K.N. Kalfas, N. Vaiana, N. Makris, A Rate-Independent Phenomenological Model for the Characterization of Pressurized Sand Dampers. *Journal of Engineering Mechanics*, **151**(**4**), 04025007, 2025.

[18] W. Ramberg, W.R. Osgood, *Description of stress-strain curves by three parameters*. Technical Note 902. National Advisory Committee on Aeronautics, Tech. Rep., 1943.

[19] M. Menegotto, Method of analysis for cyclically loaded RC plane frames including changes in geometry and non-elastic behavior of elements under combined normal force and bending. *IABSE Symposium on Resistance and Ultimate Deformability of Structures Acted on by Well Defined Repeated Loads*, International Association for Bridge and Structural Engineering: Lisbon, Portugal, 1973.

[20] R. Bouc, Forced vibrations of mechanical systems with hysteresis. *4th Conference on Nonlinear Oscillations*, Prague, Czech Republic, 1967

[21] Y. K. Wen, Approximate method for nonlinear random vibration. *Journal of the Engineering Mechanics Division*, **101**(**4**), 389-401, 1975.

[22] Y. K. Wen, Method for random vibration of hysteretic systems, *Journal of the Engineering Mechanics Division*, **102**(**2**), 249-263, 1976.

[23] H. Ozdemir, *Nonlinear transient dynamic analysis of yielding structures*. University of California, Berkeley, Berkeley, CA, 1976.

[24] N. Vaiana, S. Sessa, F. Marmo, L. Rosati, A class of uniaxial phenomenological models for simulating hysteretic phenomena in rate-independent mechanical systems and materials. *Nonlinear Dynamics*, **93**(**3**), 1647–1669, 2018.

[25] N. Vaiana, R. Capuano, S. Sessa, F. Marmo, L. Rosati, Nonlinear dynamic analysis of seismically base-isolated structures by a novel OpenSees hysteretic material model. *Applied Sciences*, **11**(**3**), 900, 2021.

[26] N. Vaiana, S. Sessa, L. Rosati, A generalized class of uniaxial rate-independent models for simulating asymmetric mechanical hysteresis phenomena. *Mechanical Systems and Signal Processing*, **146**, 106984, 2021.

[27] N. Vaiana, L. Rosati, Analytical and differential reformulations of the Vaiana–Rosati model for complex rate-independent mechanical hysteresis phenomena. *Mechanical Systems and Signal Processing*, **199**, 110448, 2023.

[28] N. Vaiana, L. Rosati, Classification and unified phenomenological modeling of complex uniaxial rate-independent hysteretic responses. *Mechanical Systems and Signal Processing*, **182**, 109539, 2023.

[29] N. Vaiana, R. Capuano, L. Rosati, Evaluation of path-dependent work and internal energy change for hysteretic mechanical systems. *Mechanical Systems and Signal Processing*, **186**, 109862, 2023.

[30] L. Cao, T. Marullo, S. Al-Subaihawi, C. Kolay, A. Amer, J.M. Ricles, R. Sause, C.S. Kusko, NHERI Lehigh experimental facility with large-scale multi-directional hybrid simulation testing capabilities. *Frontiers in Built Environment*, **6**,107, 2020.

[31] L. Cao, T. Marullo, S., J.M. Ricles, R. Sause, C. Reis, J. Sanders, Recent developments and discoveries in natural hazards mitigation research at the NHERI Lehigh Experimental Facility. *Frontiers in Built Environment*, **11**, 1567729, 2025.